Chapter 3

Previous experiments on smooth and rough walls

The present work is a continuation of the work done by Koos (2009). A detailed analysis and revision was made to this study and the revised work was published in Koos, Linares-Guerrero, Hunt, and Brennen (2012). Further experimental work has been done since then to extend the range of Stokes and Reynolds number previously studied. This is accomplished by studying liquid-solid mixtures with particles denser than the suspending liquid. Emphasis on the effects of settling and the process of particle resuspension is explored in the current work using the same experimental setup used by Koos with minor modifications to allow the visualization of the flow as described in Chapter 2.

This chapter presents the previous experimental work done on smooth and rough walls presented in Koos et al. (2012). Differences in the calibration method between the current and previous work is explained in Section 3.1. Note that parts of this chapter are taken from the paper by Koos et al. (2012).

Most of the work done by Koos et al. (2012) involved experiments where the walls of the rheometer were left smooth and the density ratio was close to one. The range of Reynolds number tested is between 20 to 800 and Stokes numbers from 3 to 90. A set of experiments with rough walls was also presented which made it possible to quantify the effect of slip at the wall by measuring the near-wall particle velocities. The depletion layer thickness, a region next to the walls where the solid fraction decreases, was calculated based on these measurements. A relation between the relative viscosity measured with rough walls and the apparent relative viscosity measured with smooth walls was given in terms of the thickness of the depletion layer. This relation has been appropriately modified and amended from the original work of Koos (2009) and it is presented in the paper of Koos et al. (2012).

3.1 Calibration

Koos (2009) measurements involved a different calibration method than the one carried out in the current experiments. The springs were calibrated in the same way as described in Section 2.2 but only during the pure fluid calibration. The subsequent torque measurements were performed without calibrating the springs nor the optic probes, since it was thought that constraining the torque measurements through the origin would overcome any uncertainty in the torque measurements. Koos considered the liquid-solid mixture flow to be Newtonian and by using the slope between points for each experiment, the intercept of the linear fit was subtracted to the corresponding data. Constraining the torque measurements through the origin will affect the recorded torque values, but will not influence the slope of the linear fit. This slope was used by Koos (2009) to find the effective viscosity of the mixture. Therefore, any error in the y-intercept in the flow curve (shear stress versus shear rate) can affect the recorded shear stress values, but does not influence the measurement of the effective relative viscosity. Constraining the torque measurements through the origin is only valid if the torque measurements are strictly linear.

A shift in the initial optic probe target can change the voltage vs displacement curve, leading to higher measurements of the torque. For the current experiments, the spring and optic probe used for each set of experiments was calibrated before and after to account for any uncertainty in the measurement of the torque and for any non-linear behavior of the flow. Moreover, the springs were pre-loaded for each experiment to account for their initial tautness and ensure their linear response.

3.2 Previous smooth walls measurements

The smooth walls experiments performed by Koos et al. (2012) involved neutrally and slightly non-neutrally buoyant particles (ρ_p/ρ goes from 1.000 to 1.009). Most of the experiments used the same polystyrene particles used in this work. Nylon and Styrene Acrylonitrile (SAN) particles were also tested by Koos. The properties of these particles are listed in table 3.1.

These particles differed in size, shape, and density, and were suspended in an aqueous glycerine solution that had a density within 0.9% of the particle density. The nylon particles were nearly spherical and about twice the size of the polystyrene ones. The styrene acrylonitrile particles were ellipsoids with a diameter close to the polystyrene particles. The random loose packing ϕ_{RLP} and the random close packing ϕ_{RCP} of each type of particle were measured in a rectangular container with a width equal to the gap in the concentric cylinder rheometer.

Figure 3.1 shows the torque measurements results of Koos (2009) for polystyrene particles for volume fractions, from 0.077 to 0.64 with a $\rho_p/\rho = 1$ and $\rho_p/\rho = 0.991$. Each point represents the mean of at least five individually recorded measurements; the error bars represent the standard

	Nylon	Polystyrene	Styrene Acrylonitrile
diameter (mm)	6.36	3.34	3.22
diameter/ gap width	0.2013	0.1057	0.1019
density (kg/m^3)	1150	1050	1070
shape	spheres	elliptical cylinders	ellipsoids
sphericity, ψ (min./max. width)	0.9999	0.7571	0.9798
RLP, ϕ_{RLP}	0.568	0.553	0.611
RCP, ϕ_{RCP}	0.627	0.663	0.657

Table 3.1: Properties of the particles used in the smooth wall experiments performed by Koos (2009). The random loose and close packing (RLP and RCP) volume fractions were measured by Koos for each type of particle.

deviation in these measurements. Linear fits for each volume fraction are also shown. The torque increases rapidly with the volume fraction, varying by several orders of magnitude between the smallest and largest volume fraction. The dependence on the volume fraction appears to be somewhat more pronounced as the volume fraction increases. The nearly linear increase in the torque with the Stokes number (and equivalently the Reynolds number for the neutrally buoyant particles, $St = \frac{1}{9}Re$) implies that the flow in these previous experiments is close to Newtonian.

The measured torque was normalized by the corresponding torque predicted from theoretical laminar flow, $M_{laminar}$. Under the assumption that the velocity distribution of the interstitial fluid is unchanged by the presence of the particles, and that the only contribution to the torque is the result of stresses from the fluid and solid phases, the ratio of the torques, M/M_f, iFrom Koos et al. (2012).s equal to the relative apparent viscosity μ_{app}/μ. Figure 3.2 presents this ratio, which is a strong function of the volume fraction and relatively independent of the Stokes number (and equivalently the Re number), except at the two lowest volume fractions ($\phi = 0.077$ and $\phi = 0.154$) where the ratio of the torques exhibits an increase at the highest Stokes number. In Koos et al. (2012), it was shown that this increase in the deviation from the mean was likely to be due to secondary flow effects. The relative apparent viscosity for the non-neutrally buoyant experiments is lower than the neutrally buoyant experiments with the same volume fraction ($\phi = 0.30$ and $\phi = 0.40$). For the non-neutrally buoyant experiments, the particles tended to float away from the test cylinder where the measurements are taken. Therefore, the actual volume fraction in the test zone may be less than the measured one. A decrease in the volume fraction would lead to a decrease in the apparent relative viscosity, which explains why the non-neutrally buoyant experiments exhibit a lower relative apparent viscosity.

Figure 3.3 shows the apparent relative viscosity results of Koos (2009) for nylon and styrene acrylonitrile particles in aqueous glycerine mixtures that matched the density of the particles.

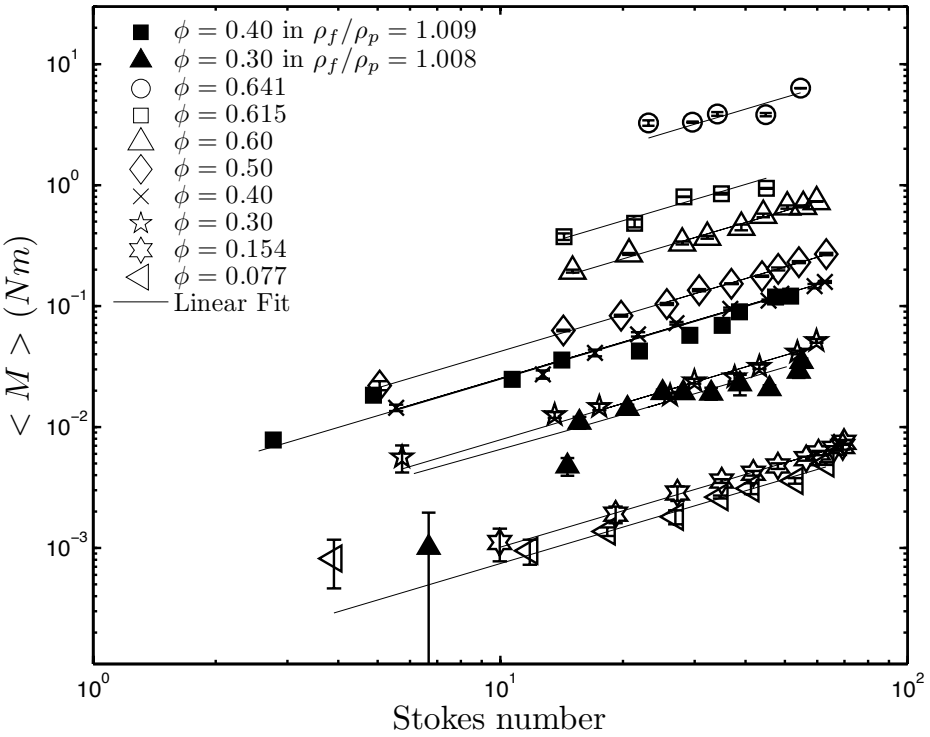

Figure 3.1: Previous torque measurements results with smooth walls. The mean measured torque ($< M >$) for suspensions of polystyrene particles in aqueous glycerine as a function of Stokes number. Closed symbols correspond to slightly non-neutrally buoyant particles. From Koos et al. (2012).

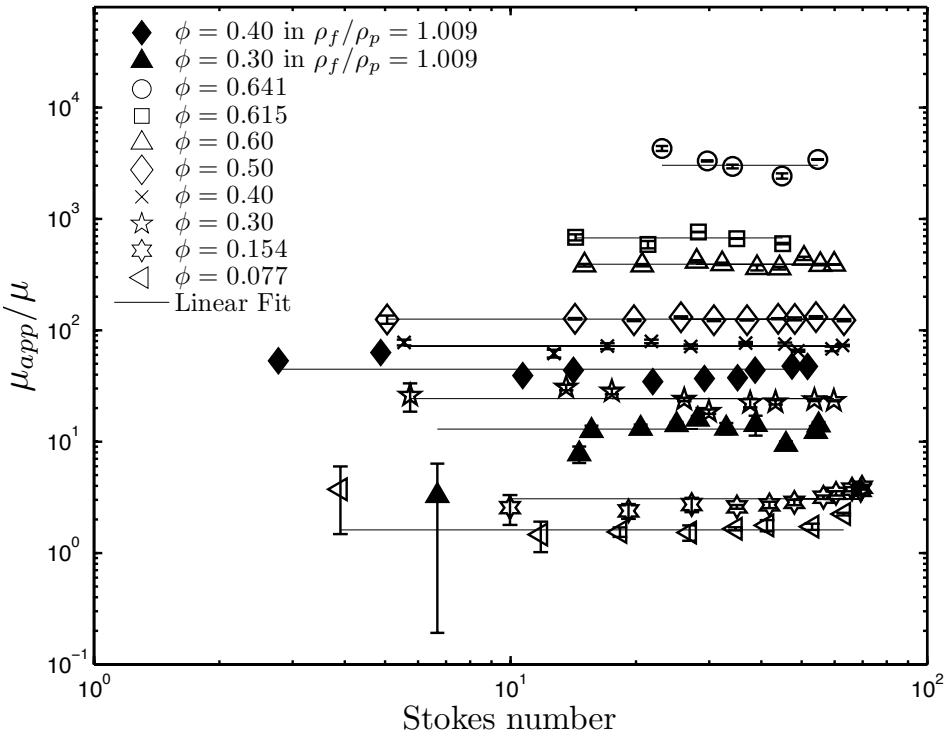

Figure 3.2: Previous normalized torques results with smooth walls. The ratio of measured to pure fluid torque (μ_{app}/μ) for suspensions of polystyrene particles in aqueous glycerine. Closed symbols correspond to non-neutrally buoyant particles. From Koos et al. (2012).

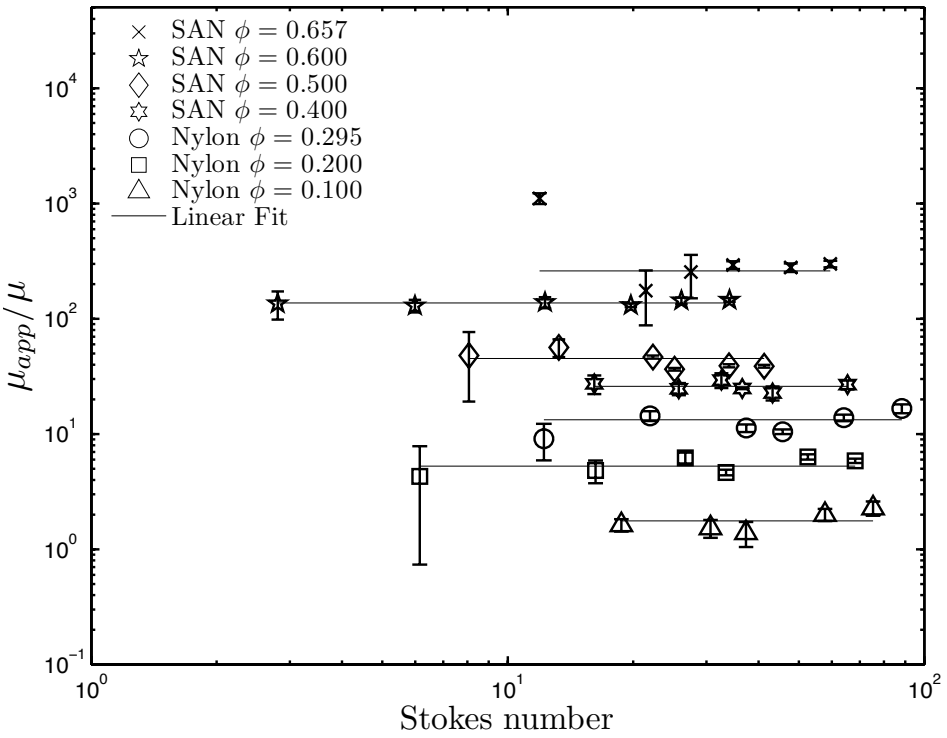

Figure 3.3: Previous results for nylon and SAN particles apparent relative viscosity (Koos et al., 2012).

The relative apparent viscosity for these experiments is also a function of the volume fraction and independent of the Stokes number except at the highest solid fraction. To compare the three experiments, the volume fraction was normalized by the random loose packing ϕ_{RLP} of each type of particles. By fitting horizontal lines to the data in Figure 3.2 and Figure 3.3 the dependence of

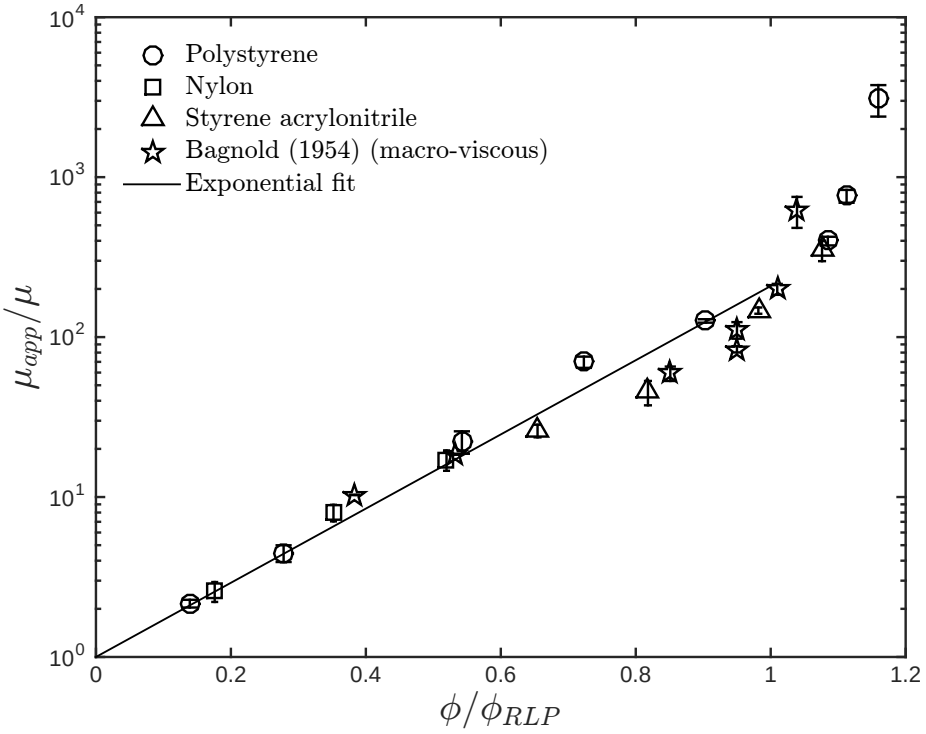

Figure 3.4: Previous results of the apparent relative viscosity for different non-settling particles in aqueous glycerine. Closed symbols correspond to non-neutrally buoyant polystyrene particles. The line is an exponential fit to the data in the region, $\phi/\phi_{RLP} < 1$. From Koos et al. (2012).

μ_{app}/μ on the volume fraction was obtained, as shown in Figure 3.4. The data in Figure 3.4 are plotted against the normalized volume fraction, ϕ/ϕ_{RLP}. Despite differences in the particle sizes and shapes, the data for all the particles tested by Koos fall along a single curve, which correlates with the volume fraction ratio.

The differences in apparent relative viscosity between $\phi > \phi_{RLP}$ and $\phi < \phi_{RLP}$ were attributed to the possible jamming of the particles. When ϕ is higher than ϕ_{RLP} the particles are not able to move past each other without deforming, which further increases the apparent viscosity. The previous smooth wall experiments show that when normalized by the size and shape dependent random loose packing fraction, ϕ_{RLP}, the relative apparent viscosity shows no dependence on the particle size or shape. Comparing the nylon to SAN particles, both have a high sphericity ($\psi = 1.00$ and 0.98), but the nylon particles are nearly twice the size of the SAN particles. Comparing the rod-shaped polystyrene particles to the nearly spherical SAN particles, there is also no difference in the measured effective viscosity. This result is different from what has been reported for low

Reynolds number suspensions, where the influence of the particles shape on the bulk viscosity has been studied (Clarke, 1967; Ward and Whitmore, 1950; Moreland, 1963). These studies showed that the more the shape of the particle deviated from that of a sphere, the greater was the bulk viscosity. Moreover, aspherical particles demonstrate increased ordering near the walls (an effect that is more pronounced for the smooth walls) (Chrzanowska et al., 2001; Börzsönyi et al., 2008).

Figure 3.4 shows the comparison between the previous smooth walls results of Koos (2009) and the previous experiments of Bagnold (1954). Only the Bagnold experiments that were free of secondary flows ($Re_b < 6,000$) are considered. The macro-viscous data from Bagnold (1954) compares favorably with the experiments of Koos (2009) and shows a similar transition at ϕ_{RLP}.

3.3 Previous rough walls experiments

Among the factors that influence the results described above is the particular structure of the liquid/solid flow at the walls of the apparatus, namely the reduction in the volume fraction near the wall and the apparent particle slip associated with that less concentrated layer. This slip is most apparent with smooth walls (Yilmazer and Kalyon, 1989; Gulmus and Yilmazer, 2007); it may lead to an erroneous mixture viscosity if a correction is not applied Barnes (2000). Experiments have shown that the slip is significantly reduced when the surface roughness is the same size as or larger than the diameter of the particles Barnes (2000). To further investigate the influence of slip on the mixture viscosity measurements, Koos performed additional experiments with rough walls using polystyrene particles. The inner and outer cylinder walls were roughened by coating them with the same polystyrene particles. The particles were glued to thin rubber sheets, which were then attached to both surfaces. The glued particles were oriented randomly and had a surface area fraction of 0.70. The decrease in gap thickness due to the rough walls was considered when calculating the shear rate for these experiments.

Figure 3.5 shows the normalized torque done by Koos (2009) with rough walls. The volume fractions tested ranged from 0.10 to 0.60. For each volume fraction, the measured torques were nearly a linear function of the Stokes number as in the case of the smooth wall data. The effective viscosity ratio increases by almost four orders of magnitude between the lowest volume fraction and the highest volume fraction. This large increase is similar to that in the smooth wall experiments.

The mean effective viscosity ratios corresponding to the horizontal lines in Figure 3.5 are plotted against the volume fraction in Figure 3.6 and compared with the smooth wall data. The large increases in the relative apparent viscosity above ϕ_{RLP} that were present in the smooth wall experiments (see Figure3.4) are not present in the rough wall data and therefore appear to be an artifact of the wall slip and depletion layers, as described in the next section. The rough wall data correlate

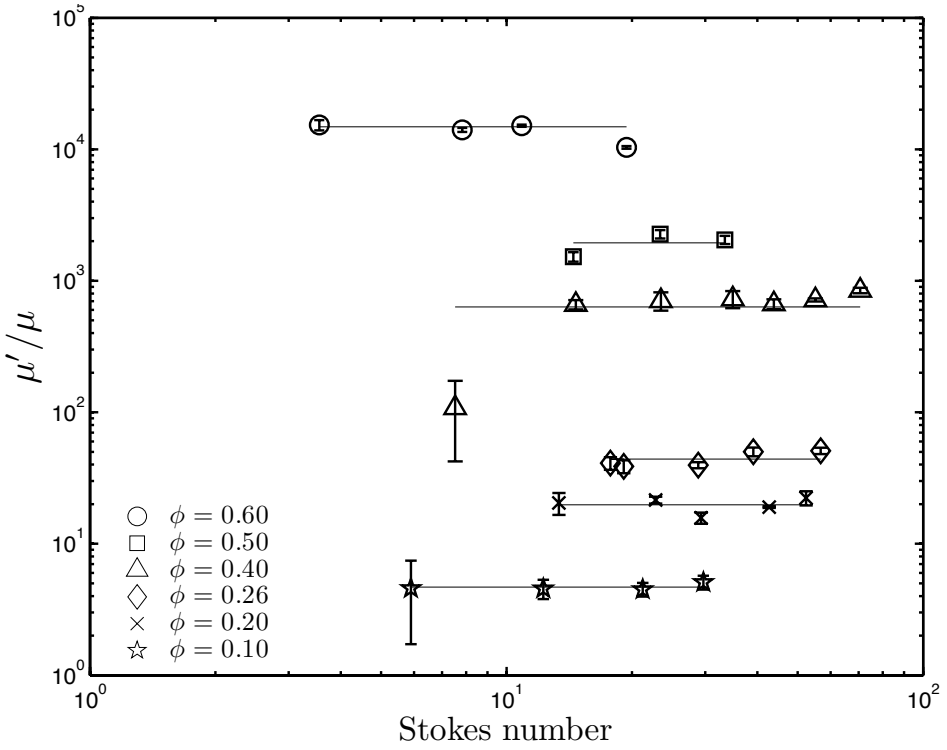

Figure 3.5: Ratio of measured torques from previous rough walls experiments. The horizontal lines are fits to the data and represent the value of the ratio of effective viscosity to pure fluid viscosity μ'/μ. From Koos et al. (2012).

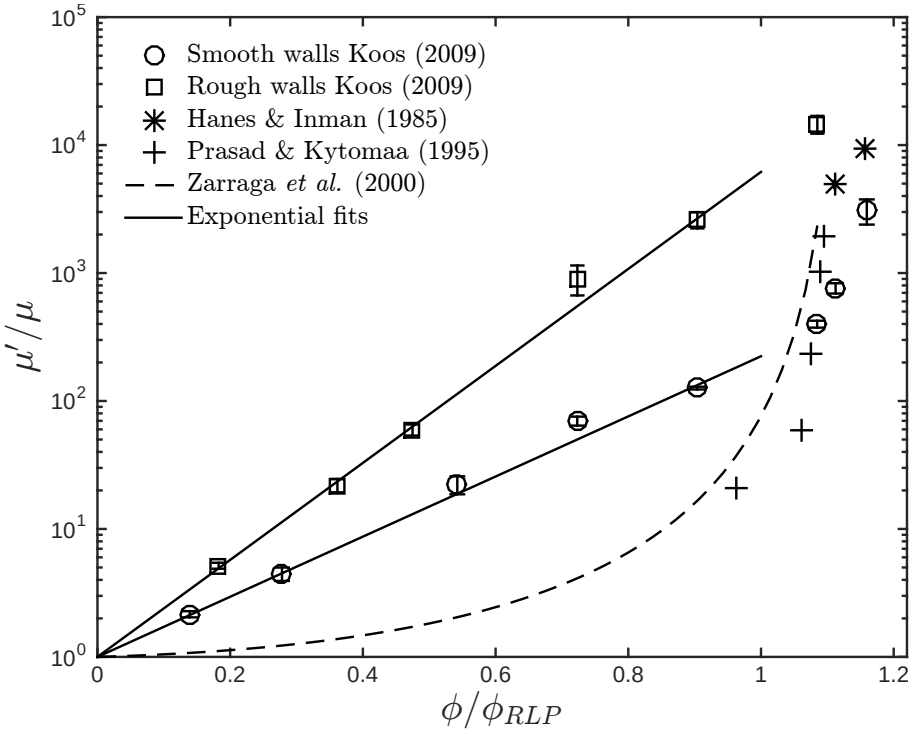

Figure 3.6: Effective viscosity ratio for neutrally buoyant polystyrene particles in aqueous glycerine solutions with rough cylinder walls. The black line is an exponential fit for the points below ϕ_{RLP}. From Koos et al. (2012).

with the volume fraction ratio and, for $\phi < \phi_{RLP}$, conform to

$$\mu'/\mu = \exp\left(8.73\frac{\phi}{\phi_{RLP}}\right), \quad \phi < \phi_{RLP}. \tag{3.1}$$

In Figure 3.4 comparison is made with the data of Hanes and Inman (1985), Prasad and Kytömaa (1995), and the empirical formula of Zarraga et al. (1999). The effective viscosities from Hanes *et al.* and Prasad *et al.* were obtained for the ratio of measured torque reported in their work and the theoretical interstitial fluid torque; their data exhibit a smaller relative effective viscosity than the current rough walls experiments. However, their experiments used settling particles; in addition, the torque was measured on the top surface of their annular gap. Hence, the torque measurements may have been affected by the migration and settling of the particles away from the top surface of the experiments. Nevertheless, the relative effective viscosities from Hanes & Inman are close to the previous data of Koos (2009). The shear rates used in their experiments were higher than those used by Prasad & Kytomaa, which may have caused a better fluidization of the suspension.

The model of Zarraga *et al.* does not fit the data of Koos. The particles used in their experiments are much smaller (of the order of microns) and therefore correspond to much lower Reynolds number ($1 \times 10^{-6} \leq Re \leq 3 \times 10^{-2}$ (Acrivos et al., 1994; Zarraga et al., 1999; Ovarlez et al., 2006; Bonnoit

et al., 2010). The apparent difference in relative effective viscosities may be due to a difference in the flow regime for this lower range of Reynolds numbers. Since particle interactions increase with Reynolds number and such interactions may cause mixing in the fluid, this could lead to an increase in the viscosity.

Depletion layer thickness

An analysis of the slip occurred with smooth walls was presented by Koos (2009). Though the interstitial fluid does not violate the no-slip condition at a solid wall, the solid particles may roll and slide, creating an effective slip (Acrivos, 1992). Slip is composed of two components. In the first component, "true slip", solid particles are able to slide over stationary walls with a non-zero velocity, creating a particle slip velocity, which is often present in granular flows (Barnes, 1995) and more marked in densely packed flows ($\phi > \phi_{RLP}$). The second component of slip, "apparent slip", is caused by the lower concentration of particles close to the walls, resulting in a lower effective local viscosity and a higher velocity gradient. Koos modeled the decrease in volume fraction near the wall by incorporating a thin depletion layer of thickness δ next to the wall in which particles are not present. This model assumes that the viscosity is uniform in both the depletion layer and the bulk core region. Amends to the model presented by Koos (2009) were done to account for algebraic mistakes. A corrected version of the model is presented in Koos et al. (2012). The model proceeds as follows. The shear stress at the inner cylinder is given by

$$\tau_i = \mu_{app} 2\omega \frac{r_o^2}{(r_o^2 - r_i^2)}, \tag{3.2}$$

where μ_{app} is the apparent viscosity of the mixture (calculated from the measured torques with smooth walls). Assuming a thin inner depletion layer devoid of particles in which the shear rate is $\dot{\gamma}_i$ it also follows that $\tau_i = \mu \dot{\gamma}_i$. Consequently, the apparent viscosity can be related to the viscosity of the two phase mixture, μ' (which is assumed to be equal to the effective viscosity measured with rough walls),

$$\mu_{app} = \frac{\mu'}{2a\left(\frac{\mu'}{\mu} - 1\right) + 1}, \tag{3.3}$$

where a is a function of the depletion layer thicknesses, δ_i and δ_o, on the inner and outer walls, respectively (see Koos et al. (2012) for derivation):

$$a = \frac{\left(\frac{\delta_i}{b} r_o^3 + \frac{\delta_o}{b} r_i^3\right)}{r_o r_i \left(r_o + r_i\right)}. \tag{3.4}$$

Previous investigations have shown that the depletion layer thickness is generally smaller than one particle diameter; its thickness increases linearly with particle diameter and, at the same volume

fraction, increases linearly with the shear stress (Soltani and Yilmazer, 1998). While these depletion layers may be smaller than a particle diameter, they can significantly change the apparent viscosity (Barnes, 2000). In addition, the radial force in a cylindrical geometry due to differences in fluid and particle densities may accentuate the depletion layer on the inner or outer cylinder surfaces. At large volume fractions, Buscall et al. (1993) and Barnes (1995) have found that the slip on the outer cylinder wall is negligible and that roughening the inner cylinder is sufficient to reduce the slip at the inner wall. Direct measurements of either the slip layer thickness or measurements of both the actual and apparent viscosities are needed to quantify this error.

Using the values of the smooth (apparent) and the rough (effective) viscosity data of Figure 3.6, the function a and the depletion layer thickness can be calculated for each volume fraction. Figure 3.7 shows the depletion layer thicknesses calculated using the smooth walls data from Koos (2009) and assuming that slip occurs either on the inner cylinder alone or that the depletion thicknesses are the same on both the inner and outer cylinders. Typical depletion layer thicknesses derived

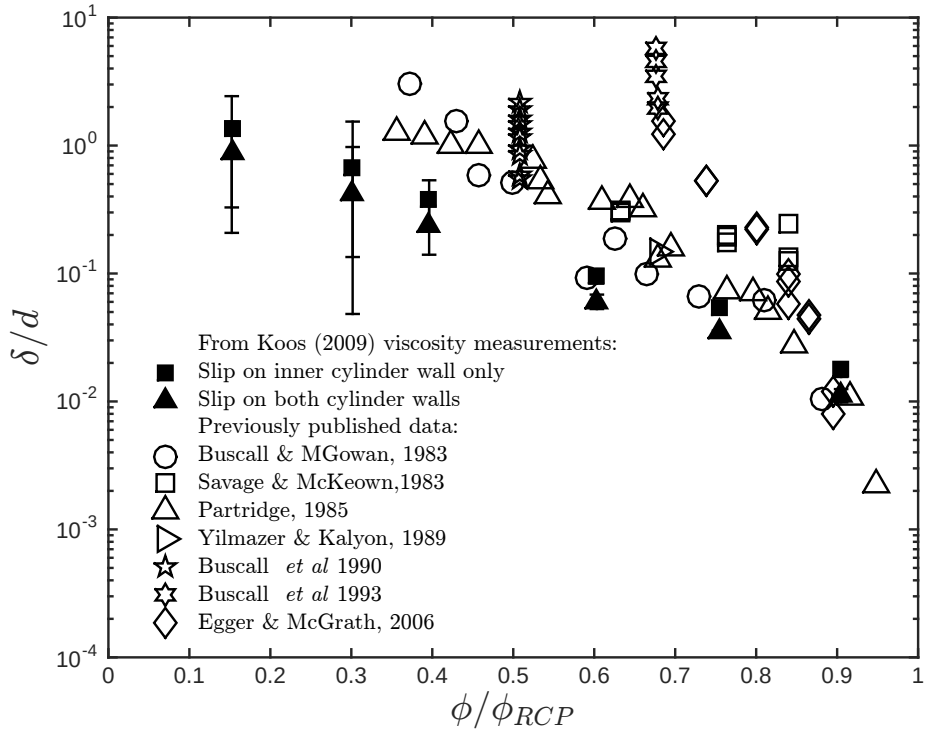

Figure 3.7: Depletion layer thicknesses (divided by the particle diameter) calculated from previous apparent and effective viscosity measurements of Koos (2009), using equation 3.3 (closed symbols) as a function of the volume fraction ratio ϕ/ϕ_{RCP}, where ϕ_{RCP} is the random close packing. The error bars account for the standard deviation in the torque measurements. Also shown are typical depletion layer thicknesses on the inner cylinder of concentric cylinder devices from references (Buscall et al. (1993); Savage and McKeown (1983); Yilmazer and Kalyon (1989); Buscall et al. (1993); Partridge (1985); Buscall et al. (1990); Egger and McGrath (2006) (open symbols).

from previously reported data are also shown in figure 3.7. The random close packing was used to

normalized the volume fraction. The Savage and McKeown shear stress measurements data with smooth and rough wall were used to calculate the depletion layer thickness by using equation 3.3 and assuming slip on the inner cylinder only. Savage and McKeown (1983) used polystyrene beads $d \approx 1$ mm particles that are approximately the same size as the ones used in the rough wall experiments of Koos. Egger and McGrath data for a $d \approx 0.5$ μm emulsion were obtained by considering slip on both cylinders and following a different approach described by the authors and discussed later in this section. The rest of the data in figure 3.7 were calculated from shear stress measurements for $d \approx 1$ μm polystyrene beads as reported in Buscall et al. (1993) and considered slip only on the inner cylinder. The calculated depletion layer thickness from the data of Koos is close to, though slightly less than, previously recorded data. This may due to the fact that Egger and McGrath (2006) and Buscall et al. (1993) considered a more idealized scenario. Egger and McGrath followed the approach made by Russel and Gran (2000) where they assumed that the applied shear stress at a given radius is uniform over the whole sample. Egger and McGrath validated this assumption by the closeness in the mapping of their rough wall data and the slip corrected data. Buscall et al. (1993) assumed that the actual viscosity (which they called true viscosity) is large enough so its inverse value can be neglected. With the data of Koos, there is little difference between the predicted values using slip on the inner wall or on both walls, though the assumption of slip in the inner wall alone results in a better match to previously recorded data.

Slip velocity measurements

The depletion layer on the inner cylinder can also be estimated from particle velocities measurements. Koos (2009) evaluated the velocities of the particles next to the inner cylinder by using a pair of MTI fiber-optic proximity probes that were installed flush with the surface of the inner cylinder at an observation port 2.86 cm below the test cylinder. These were used to both count the particles passing the probe and, by cross-correlation, to measure the velocity of those particles. The cross correlation was done over a full ten seconds to find the mean particle velocity and the measurement of individual particle velocities.

Using the velocities measurements performed by Koos, and assuming that there are no particles in the depletion layer and that the particles viewed by the optical probes are those at the depletion layer-core region interface, the interfacial velocity, u, at $r = r_i + \delta_i$ is given by

$$\frac{u}{\omega r_o} = \frac{2\delta_i r_o}{r_o^2 - r_i^2} \frac{\mu_{app}}{\mu}, \tag{3.5}$$

(see Koos et al. (2012) for derivation) and this can be used along with the measured particle velocities, u, to obtain estimates of the depletion layer thickness, δ_i. Figure 3.8 shows the calculated thicknesses as a function of Stokes number and volume fraction. Note that the thickness is relatively independent

of Stokes number but varies substantially with the volume fraction. The same data is included in Figure 3.9, where it is seen to be consistent with the values derived from the present rheological measurements. Note that the estimates for the depletion layer thickness fall slightly below previously published data for volume fractions below ϕ_{RLP}. This deviation can be explained by the ordering of particles next to the walls. Specifically, the surface area oriented towards the optic probes fluctuates as a function of the distance from the wall Chen and Louge (2008). These fluctuations can give rise to errors in the measurements of the particle velocity. In the previous experiments of Koos (2009), the orientation of the particles should result in the depletion layer thickness being underestimated.

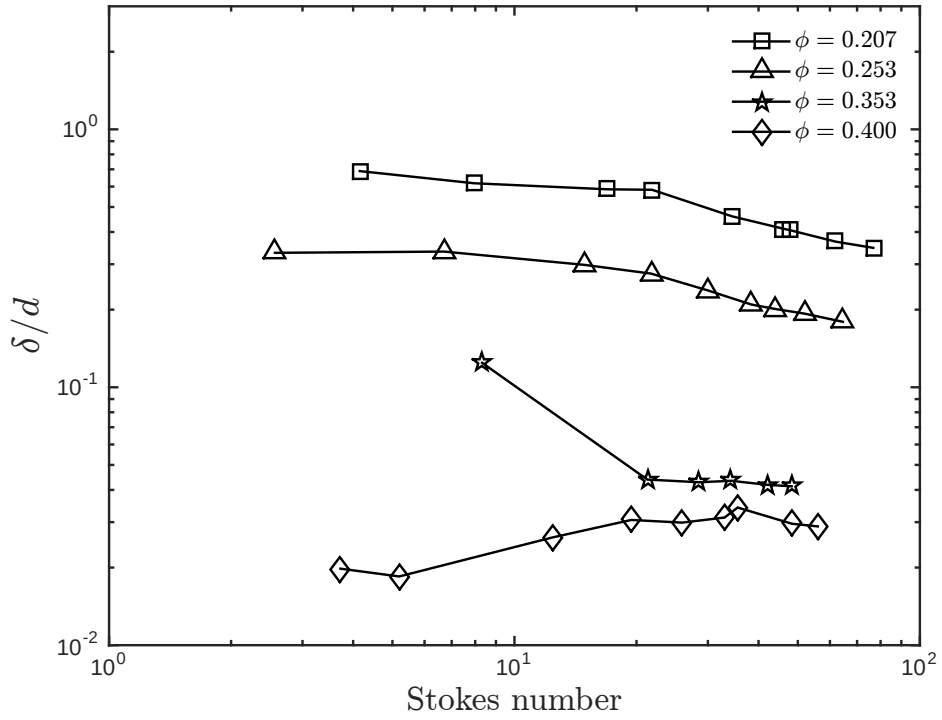

Figure 3.8: Depletion layer thicknesses (δ) calculated from Koos (2009) particle velocity measurements as a function of Stokes number for several volume fractions. From Koos et al. (2012).

3.4 Summary

The previous work covered a range of moderate Stokes number (from 3 to 90). For the smooth walls three different types of particles were tested. Despite differences in the particle materials, sizes, and shapes, the data for all tested particles correlate with the volume fraction ratio for $\phi < \phi_{RLP}$. A slight mismatch in the fluid and particle density (within 1%) does not change the dependency of the apparent viscosity on the volume fraction ratio ϕ/ϕ_{RLP}.

In the "rough wall" experiments only one type of particles was tested. These particles were glued to both the inner and outer cylinder walls. This configuration appears to result in appropriate

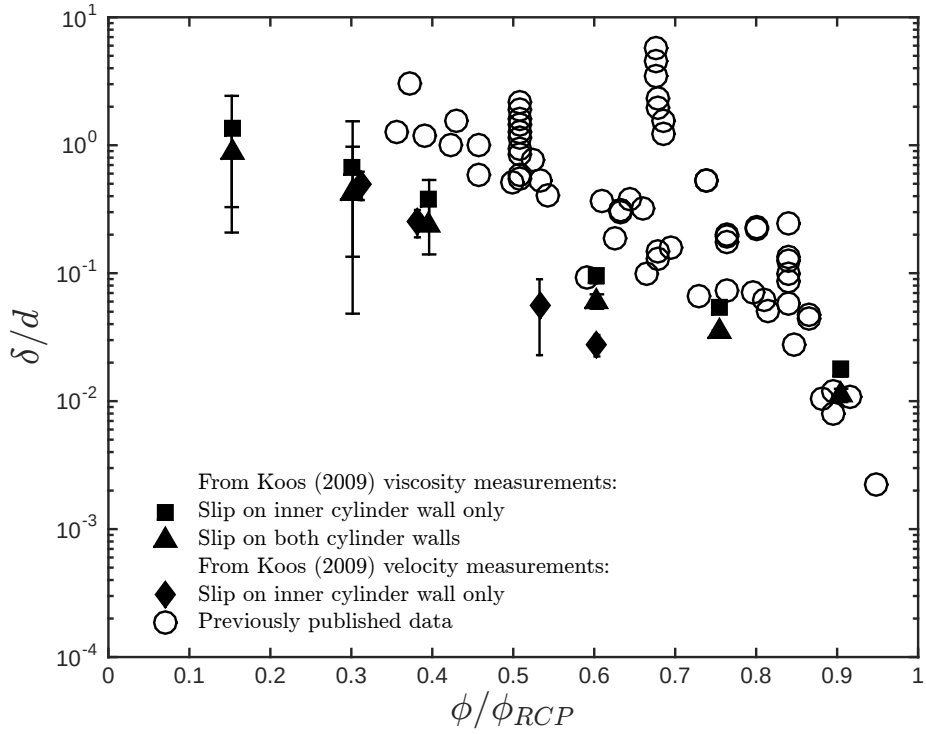

Figure 3.9: Depletion layer thicknesses calculated from previous measurements of the apparent and effective viscosity using equation 3.3 and depletion thicknesses calculated from the velocity measurements using equation 3.5. Also shown are the previously reported experimental values from figure 3.7. From Koos et al. (2012).

effective mixture viscosities that increase exponentially with the volume fraction up to the loose packed volume fraction. On the other hand, the measurements with smooth wall cylinders clearly demonstrate that wall slip substantially affects the apparent viscosity. The slip was modeled by assuming thin depletion layers on the smooth walls. The thickness of the depletion layers was estimated by measuring the particle velocities near the walls. In addition the values for the rough and smooth wall viscosities were used to evaluate the thickness of the depletion layer over the full range of volume fractions. From these two methods the resulting depletion layer thicknesses are shown to be in agreement with previous investigations. For volume fractions less than the loose packed volume fraction, ϕ_{RLP}, the slip is caused by thin depletion layers that decrease in thickness as the volume fraction is increased. For $\phi > \phi_{RLP}$, slip caused by particles sliding over the cylinder walls appears to dominate and contributes significantly to the differences between the smooth and rough wall measurements.

The previous torque measurements for rough and smooth walls scale linearly with the shear rate and only the experiments with volume fractions lower than 20% exhibited a deviation from the linear behavior at high Stokes numbers. Such deviation is likely to be due to inertial effects of the suspending liquid. In this previous study, evidence of particle interaction's effect on the scaling of the shear stress with the shear rate was not observed. However, the measured relative viscosities are higher than the previous experiments, which may result from the induced mixing of the fluid due to particle interactions.